J. Braz. Chem. Soc., Vol. 21, No. 1, S1-S18, 2010.
Printed in Brazil - ©2010 Sociedade Brasileira de Química
0103 - 5053 $6.00+0.00

Novel 2-(R-phenyl)amino-3-(2-methylpropenyl)-[1,4]-naphthoquinones: Synthesis, Characterization, Electrochemical Behavior and Antitumor Activity

Acácio I. Francisco,[a] Annelise Casellato,[a#] Amanda P. Neves,[a] J. Walkimar de M. Carneiro,[a] Maria D. Vargas,*,[a] Lorenzo do C. Visentin,[b] Alviclér Magalhães,[c] Celso A. Câmara,[d] Claudia Pessoa,[e] Letícia V. Costa-Lotufo,[e] José D. B. Marinho Filho[e] and Manoel O. de Moraes[e]

[a]*Instituto de Química, Universidade Federal Fluminense, 24020-141 Niterói-RJ, Brazil*

[b]*Instituto de Química, Universidade Federal do Rio de Janeiro, 22640-000 Rio de Janeiro-RJ, Brazil*

[c]*Instituto de Química, Universidade Estadual de Campinas, 13083-970 Campinas-SP, Brazil*

[d]*Instituto de Química, Universidade Federal Rural de Pernambuco, 52171-900 Recife-PE, Brazil*

[e]*Departamento de Fisiologia e Farmacologia, Universidade Federal do Ceará, 60430-270 Fortaleza-CE, Brazil*

1. Theoretical Calculations

Starting from the experimental structure for **2b** (4-Me), the geometries of **2a**-**2e** and **2h**-**2i** were fully optimized with the B3LYP/6-31G(d) method. Energies and molecular properties were obtained from a single-point calculation using the 6-311+G(2d,p) basis set and the B3LYP functional. To confirm that the most stable conformation in the gas-phase is similar to that found in the solid state the geometry of an alternative conformation for **2b**, with the 2-methyl-propenyl group bonded to the position 3 of the naphthoquinone ring rotated by 180º was also optimized. This alternative conformation was found 0.4 kcal mol^{-1} less stable than the solid state conformation. The barrier for conversion between the two conformers calculated at the 6-31G(d) level is 5.5 kcal mol^{-1}.

The orientation of the 2-phenylene ring is stabilized by an intramolecular hydrogen bond with one carbonyl group of the naphthoquinone ring and was, therefore, not further investigated. NMR absolute chemical shifts were calculated using the GIAO (Gauge Independent Atomic Orbital) method with the B3LYP/6-311+G(2d,p) approach on the B3LYP/6-31G(d) optimized geometry. Absolute energies and GIAO nuclear magnetic shielding tensors for H(18) are given in Table S1. Interestingly, the δ_{H18} value for the alternative conformation (with the 2-methyl-propenyl group rotated by 180º, entry **2b**-4 in Table S1) is 1.67 ppm shifted highfield as compared to the same hydrogen in the most stable conformation. Calculation for **2b** on a geometry with the methoxy group rotated by 90º (entry **2b**-2 in Table S1) yielded essentially the same δ_{H18} value as that obtained for the most stable conformation. To verify the effect of the solvent on the chemical shifts some calculations were repeated with the solvent chloroform, using the CPCM approach. These calculations revealed that the solvent has only marginal influence on the relative chemical shifts.

The electronic spectra were calculated using the TD (Time Dependent) methodology available in Gaussian. The PBE1PBE functional together with the 6-311+G(2d,p) basis set was employed. All calculations were carried out with the G03W package of molecular orbital calculation.

2. Crystallographic Data

2.1. Computing details

Data collection: *COLLECT* (Nonius, 1998); cell refinement: *PHICHI* (Duisenberg, 2000); data reduction: *EVALCCD* (Duisenberg, 2003); program(s) used to solve structure: *SHELXS97* (Sheldrick, 1997); program(s) used to refine structure: *SHELXL97* (Sheldrick, 1997); molecular graphics: *ORTEP-3 for Windows* (Farrugia, 1997); software used to prepare material for publication: *WinGX* publication routines (Farrugia, 1999).

2.2. Experiment X-ray diffraction

The X-ray diffraction data for (**2b**) were collected at 295 K from a *Enraf-Nonius Kappa*-CCD diffractometer with graphite-monochromatized Mo K_α radiation. The cell parameters were obtained and refined using *PHICHI* and

*e-mail: *e-mail: mdvargas@vm.uff.br
#Present address: Instituto de Química, Universidade Federal do Rio de Janeiro, 22640-000 Rio de Janeiro-RJ, Brazil

Table S1. Absolute energies (Hartree) and GIAO nuclear magnetic shielding tensors (ppm) for compounds **2a**-**2e** and **2h**-**2i**. All calculations were carried out on a optimized B3LYP/6-31G(d) geometry

	Absolute energies / hartree		GIAO nuclear magnetic shielding tensors / ppm	
Derivative	B3LYP/6-31+G(d,p)	B3LYP/6-311+G(2d,p)	B3LYP/6-31+G(d,p)[a]	B3LYP/6-311+G(2d,p)[b]
2a (H)	-977.62466	-	24.64	-
2b-1 (4-OMe)	-1092.15228	-1092.40283	24.64	24.97
2b-2 (4-OMe)[c]	-1092.14589	-	24.67	-
2b-3 (4-OMe)[d]	-1092.16808	-	24.64	-
2b-4 (4-OMe)[e]	-1092.16687	-	26.31	-
2l (3-OMe)	-1092.15346	-1092.40399	24.62	24.89
2c (4-Fc)	-2627.17389	-2627.55599	24.66	24.79
2m (3-Fc)	-	-2627.55562	-	24.85
2d (4-Me)	-1016.94536	-1017.17288	24.60	24.86
2e (3-Me)	-	-1017.17322	-	24.81
2h-1 (4-CN)	-1069.87032	-1070.11410	24.50	24.79
2h-2 (4-CN)[d]	-1069.89020	-	24.46	-
2i-1 (3-CN)	-1069.86851	-1070.11232	24.54	24.75
2i-2 (3-CN)[d]	-1069.88800	-	24.49	-

[a]At this level, the absolute GIAO nuclear magnetic shielding of TMS is 32.09 ppm. [b]At this level, the absolute GIAO nuclear magnetic shielding of TMS is 31.82 ppm. [c] Conformation with the methoxy group rotated by 90º. [d]Calculation with inclusion of solvent (CPCM, chloroform). The absolute GIAO nuclear magnetic shielding of TMS at this level is 31.63 ppm [e]Alternative conformation, with the 2-methyl-propenyl group rotated by 180º, including solvent effect (chloroform).

EvalCCD programs. Intensities for (**2b**) were corrected by Lorentz polarization and absorption with the *SADABS* program. The structure was solved by *SHELXS*-97 Direct Methods, and refined with *SHELXL*-97, contained within the *WinGX*-32 crystallography program. The positional parameters of the H atoms bonded to C atoms in the phenyl rings were obtained geometrically, with the C-H distances fixed in 0.93Å for Csp^2, and refined as riding on their respective C atoms, with U_{iso}(H) = 1.2Ueq(Csp^2). H atoms bonded to C atoms in the methyl group were located geometrically and with the C-H distances fixed at 0.96Å for Csp^3 and with U_{iso}(H) = 1.5Ueq(Csp^3). The positional parameters of H(1) bonded to N(1) was obtained from a Fourier difference map and refined freely with an isotropic displacement parameter; the distance for N(1)-H(1) is 0.87(2). X-ray data are listed in Table S2.

Crystallographic data for the structural analysis of compound **2b** have been deposited with the Cambridge Crystallographic Data Center, CCDC 734112. Copies of this information may be obtained free of charge from The Director, CCDC, 12 Union Road, Cambridge, CB2 1EZ, UK (fax: +44 1233336 033; e-mail: deposit@ccdc.cam.ac.uk).

The packing of **2b** involves molecules that interact intra- and intermolecularly through classical and non-classic hydrogen bonds, forming a 1D infinite network along the [100] crystallographic direction (Figures S2 and S3). The naphthoquinone carbonyl O1^{i} interacts *via* classical and non-classic hydrogen bonds with H(1) to N(1) (imine group) and with H(12) to C(12) [C(11)-C(16) phenyl ring] of a neighboring molecule forming a six membered ring [symmetry code: $i = x-1, y, z$]. In addition the other carbonyl group interacts *via* O2^{ii} with H(5) to C(5) forming a ten membered ring in association with N(1)-H(1)···O(1). The H-bond geometric parameters are listed in Table S4. Table S5 gathers the atomic coordinates and equivalent isotropic displacement parameters.

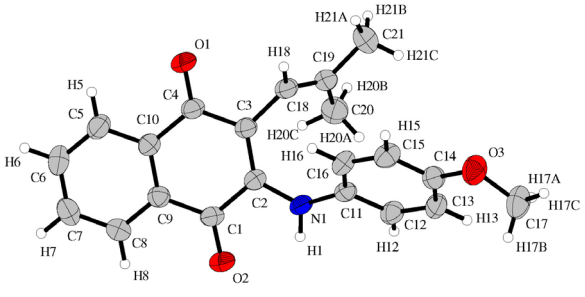

Figure S1. View of the ORTEP plot for **2b** with labeled atoms and 50% probability ellipsoids.

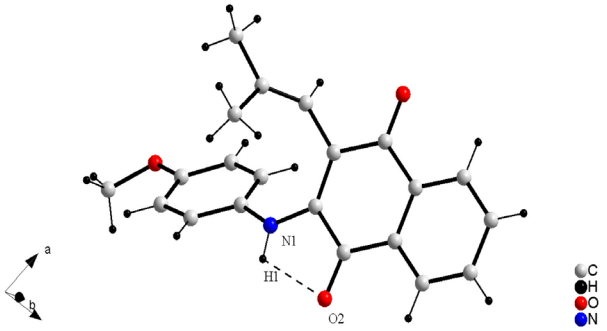

Figure S2. View of the intramolecular interaction.

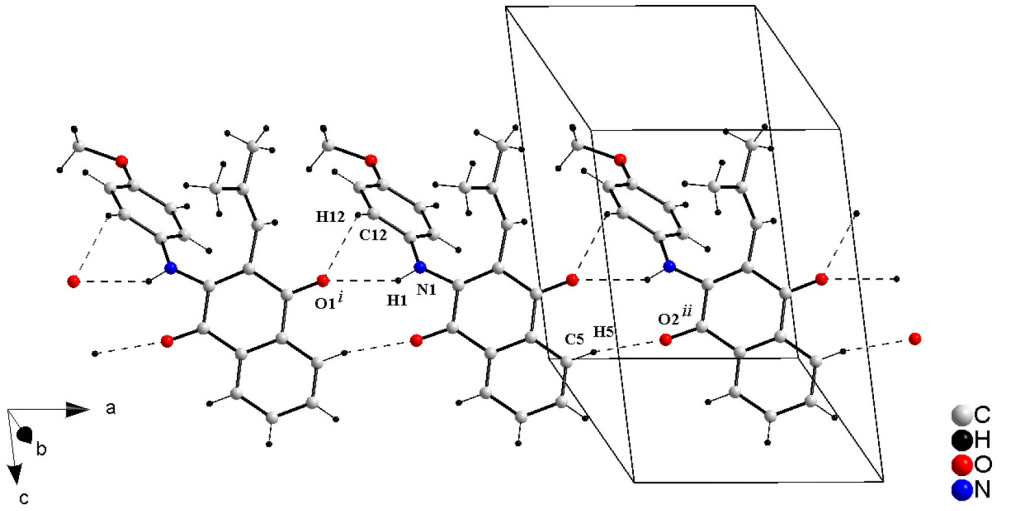

Figure S3. View of the self-assembly 1D by classical and non classical hydrogen bonds along the [100] crystallography direction. [Symmetry codes: (*i*) *x*–1, *y*, *z*; (*ii*) *x*+1, *y*, *z*].

Table S2. Crystal data and structure refinement for **2b**.

Formula	$C_{21}H_{19}O_3N$
formula weight	333.37
crystal system, space group	Triclinic, P-1
crystal size / mm	0.30 x 0.20 x 0.15
a /Å	7.8709(16)
b/Å	9.3748(19)
c/Å	12.117(2)
α / (°)	86.11(3)
β / (°)	81.60(3)
γ / (°)	78.26(3)
V / Å^3	865.3(3)
Z	2
T / K	295
$\rho_{calc.}$ / (g cm^{-3})	1.279
μ / mm^{-1}	0.086
2θ range	3.99 to 25.00
F(000)	352
Reflections collected	10324
Reflections unique	3023
R_{int}	0.0358
Max. and min. transmission	0.9873 and 0.9748
data[b]/restraints/parameters	3023 / 0 / 232
S[b,c]	1.027
R_1[a,d]	0.0430
wR_2[b,e]	0.1031
largest difference peak and hole / (e Å^{-3})	0.153 and -0.180

[a] $F_o^2 \geq 2\sigma(F_o^2)$. [b] $F_o^2 \geq 3\sigma(F_o^2)$. [c] $S = [\Sigma w(F_o^2 - F_c^2)^2/(n-p)]^{1/2}$. [d] $R_1 = \Sigma||F_o| - |F_c||\Sigma|F_o|$. [e] $wR_2 = [\Sigma w(F_o^2 - F_c^2)^2/\Sigma w(F_o^4)]^{1/2}$

Table S3. Geometric parameters for molecule **2b** (Å, °)

Bonds distances	
N(1)-C(11)	1.424(2)
N(1)-C(2)	1.367(2)
O(1)-C(4)	1.234(2)
O(2)-C(1)	1.223(2)
O(3)-C(14)	1.378(2)
O(3)-C(17)	1.423(2)
C(3)-C(18)	1.480(2)
C(19)-C(18)	1.328(3)
C(19)-C(20)	1.502(3)
C(19)-C(21)	1.510(3)
Bond angles	
C(2)-N(1)-C(11)	129.43(15)
C(14)-O(3)-C(17)	116.93(16)
O(1)-C(4)-C(3)	120.81(16)
O(1)-C(4)-C(10)	119.19(16)
O(2)-C(1)-C(9)	121.52(16)
O(2)-C(1)-C(2)	119.54(16)
C(19)-C(18)-C(3)	126.38(17)
C(20)-C(19)-C(21)	115.62(18)

Table S4. Geometric parameters for non-classical H bonds for molecule (**2b**) (*Å*, °)

D-H···A	*D*-H	H···A	*D*···A	∠*D*-H···A
N(1)—H(1) ···O(2)	0.87 (2)	2.18 (2)	2.620 (2)	111.2 (18)
N(1)—H(1) ···O(1)^i	0.87 (2)	2.46 (2)	3.241 (2)	150.2 (18)
C(12)—H(12)···O(1)^i	0.93	2.58	3.246 (2)	129
C(5)—H(5) ···O(2)^{ii}	0.93	2.39	3.304 (2)	169

[Symmetry codes: (*i*) *x*-1, *y*, *z*; (*ii*) *x*+1, *y*, *z*]

Table S5. Atomic coordinates (× 10^4) and equivalent isotropic displacement parameters (A^2 × 10^3) for (**2b**). U(eq) is defined as one third of the trace of the orthogonalized *Uij* tensor

	x	y	z	U(eq)
C(19)	–974(2)	–1627(2)	5732(2)	43(1)
C(20)	–2387(3)	–494(2)	5299(2)	52(1)
C(21)	–31(3)	–2776(3)	4922(2)	70(1)
O(1)	1355(2)	–120(2)	7804(1)	54(1)
O(2)	–5563(2)	1227(2)	9030(1)	54(1)
C(2)	–3178(2)	–323(2)	8018(1)	33(1)
N(1)	–4432(2)	–1001(2)	7743(1)	38(1)
C(1)	–3973(2)	916(2)	8784(1)	36(1)
C(9)	–2800(2)	1709(2)	9233(1)	35(1)
O(3)	–4254(2)	–6772(1)	6747(1)	57(1)
C(10)	–984(2)	1312(2)	8931(1)	35(1)
C(4)	–239(2)	152(2)	8106(2)	36(1)
C(3)	–1409(2)	–604(2)	7634(1)	34(1)
C(11)	–4275(2)	–2456(2)	7413(1)	34(1)
C(12)	–5544(2)	–2751(2)	6832(2)	40(1)
C(18)	–559(2)	–1641(2)	6757(2)	39(1)
C(16)	–2999(2)	–3610(2)	7728(2)	40(1)
C(8)	–3498(2)	2840(2)	9955(2)	44(1)
C(14)	–4310(2)	–5325(2)	6920(2)	39(1)
C(15)	–3008(2)	–5025(2)	7473(2)	43(1)
C(5)	112(2)	2050(2)	9372(2)	44(1)
C(13)	–5574(2)	–4176(2)	6589(2)	43(1)
C(6)	–601(3)	3166(2)	10106(2)	51(1)
C(7)	–2398(3)	3565(2)	10390(2)	51(1)
C(17)	–5788(3)	–7133(2)	6440(2)	61(1)

3. ^{1}H NMR and APT Spectra ($CDCl_3$) of Compounds 2a-k

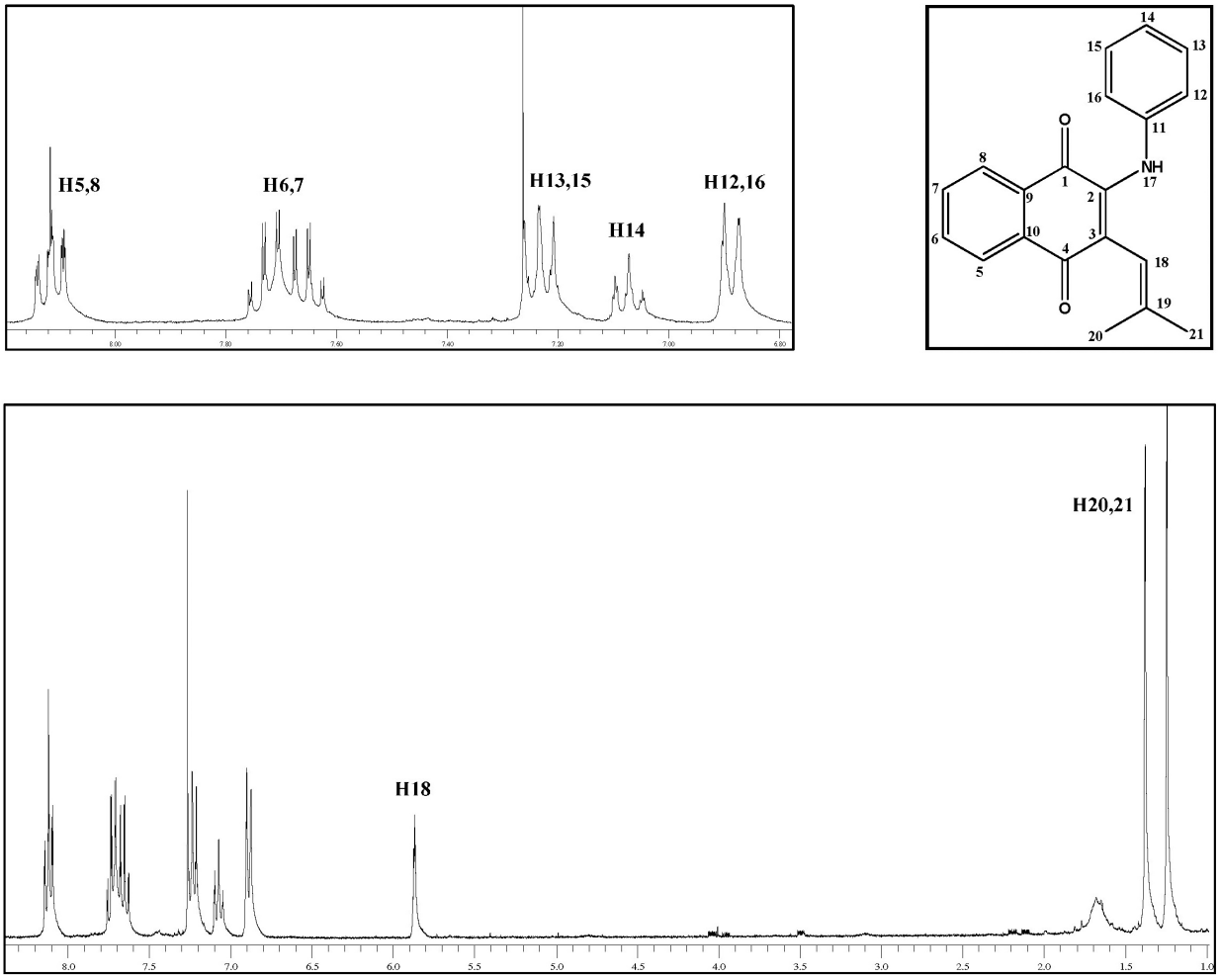

Figure S4. ^{1}H NMR spectrum of 2-(phenyl)amino-3-(2-methylpropenyl)-1,4-naphthoquinone (**2a**).

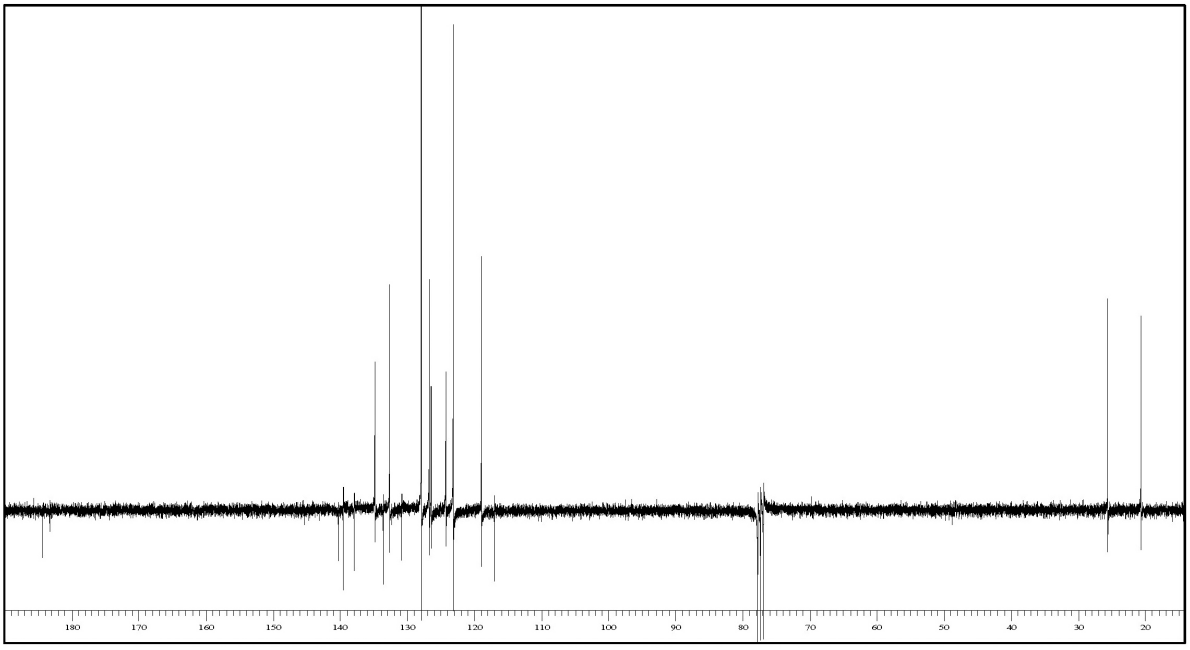

Figure S5. APT spectrum of 2-(phenyl)amino-3-(2-methylpropenyl)-1,4-naphthoquinone (**2a**).

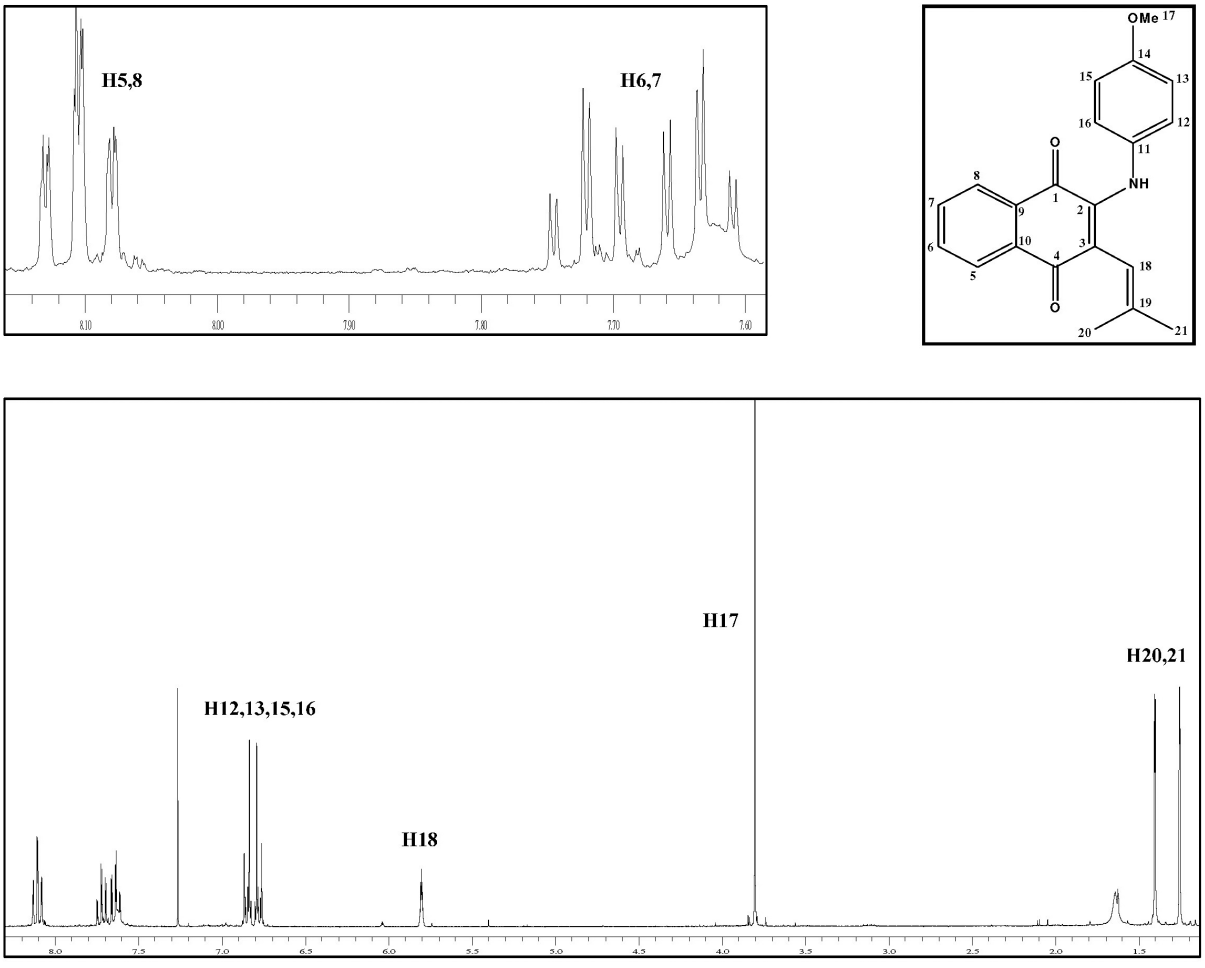

Figure S6. ^{1}**H NMR** spectrum of 2-(4-methoxy-phenyl)amino-3-(2-methylpropenyl)-1,4-naphthoquinone (**2b**).

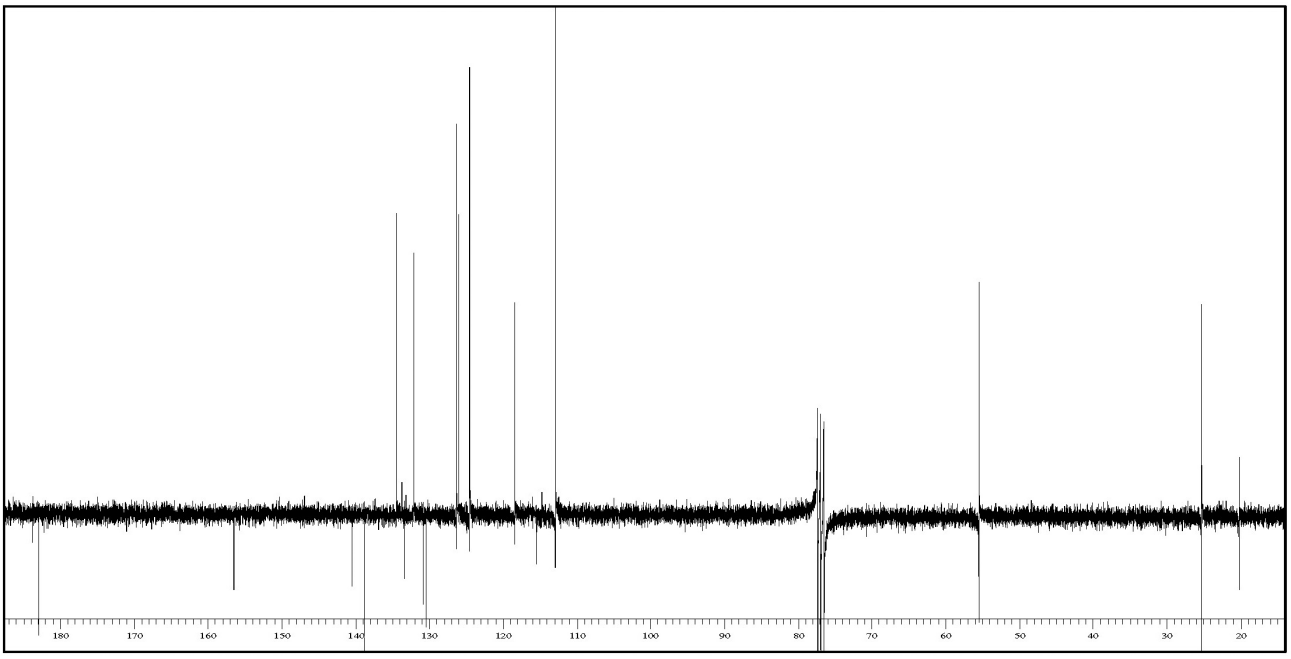

Figure S7. APT spectrum of 2-(4-methoxy-phenyl)amino-3-(2-methylpropenyl)-1,4-naphthoquinone (**2b**).

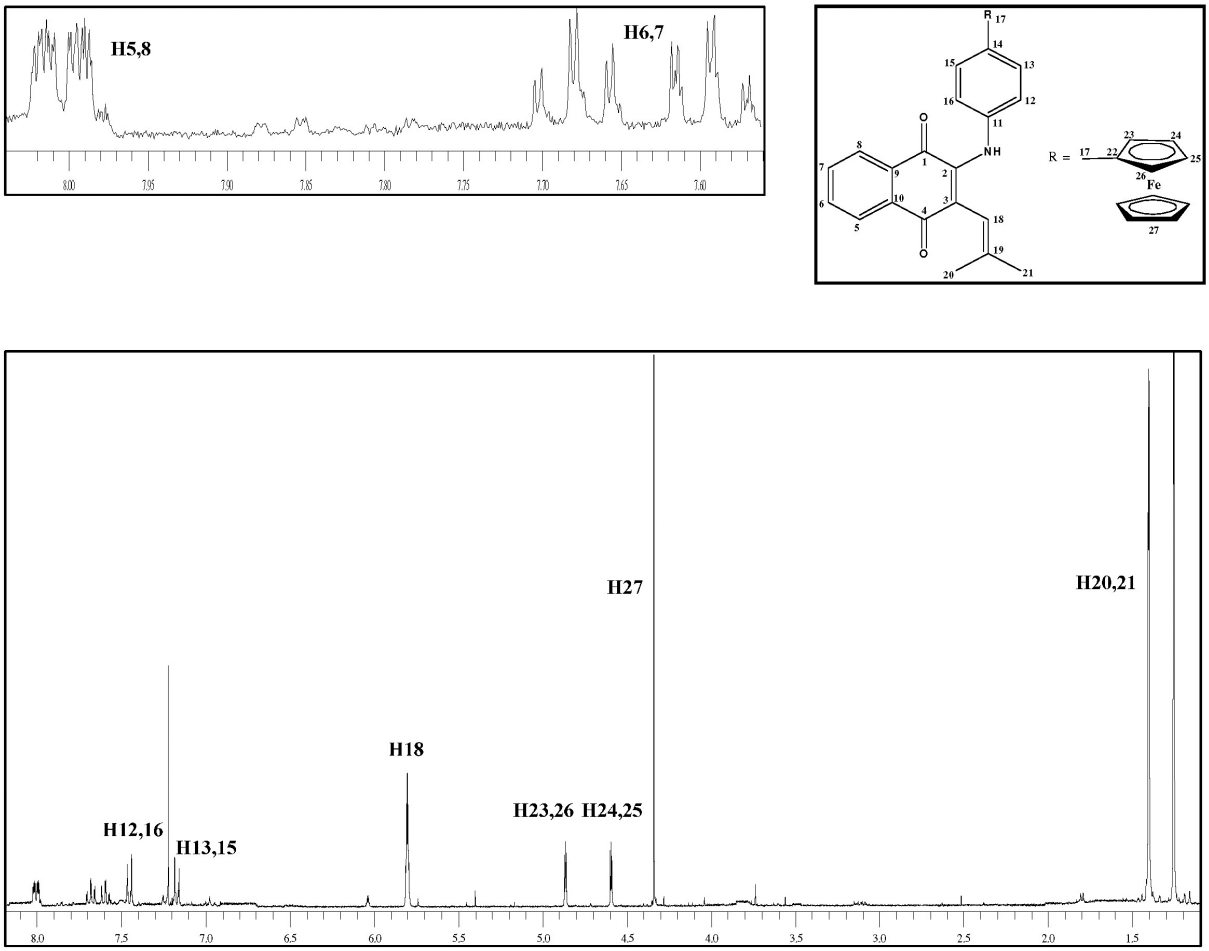

Figure S8. ^{1}H NMR spectrum of 2-(4-ferrocenyl-phenyl)amino-3-(2-methylpropenyl)-1,4-naphthoquinone (**2c**).

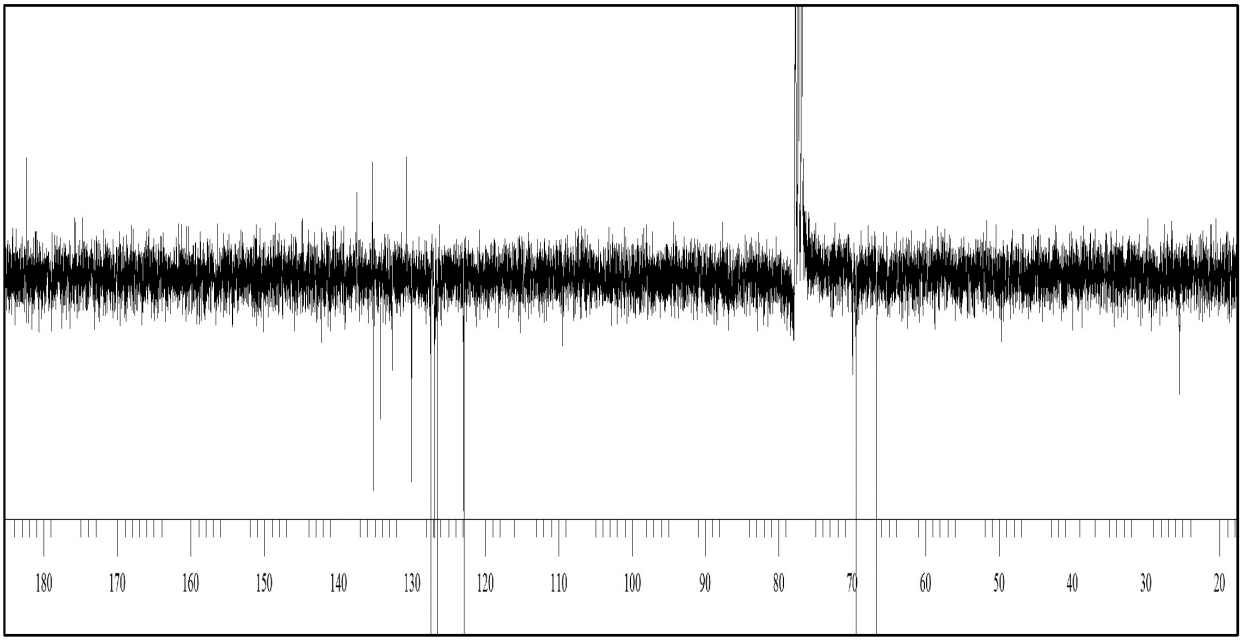

Figure S9. APT spectrum of 2-(4-ferrocenyl-phenyl)amino-3-(2-methylpropenyl)-1,4-naphthoquinone (**2c**).

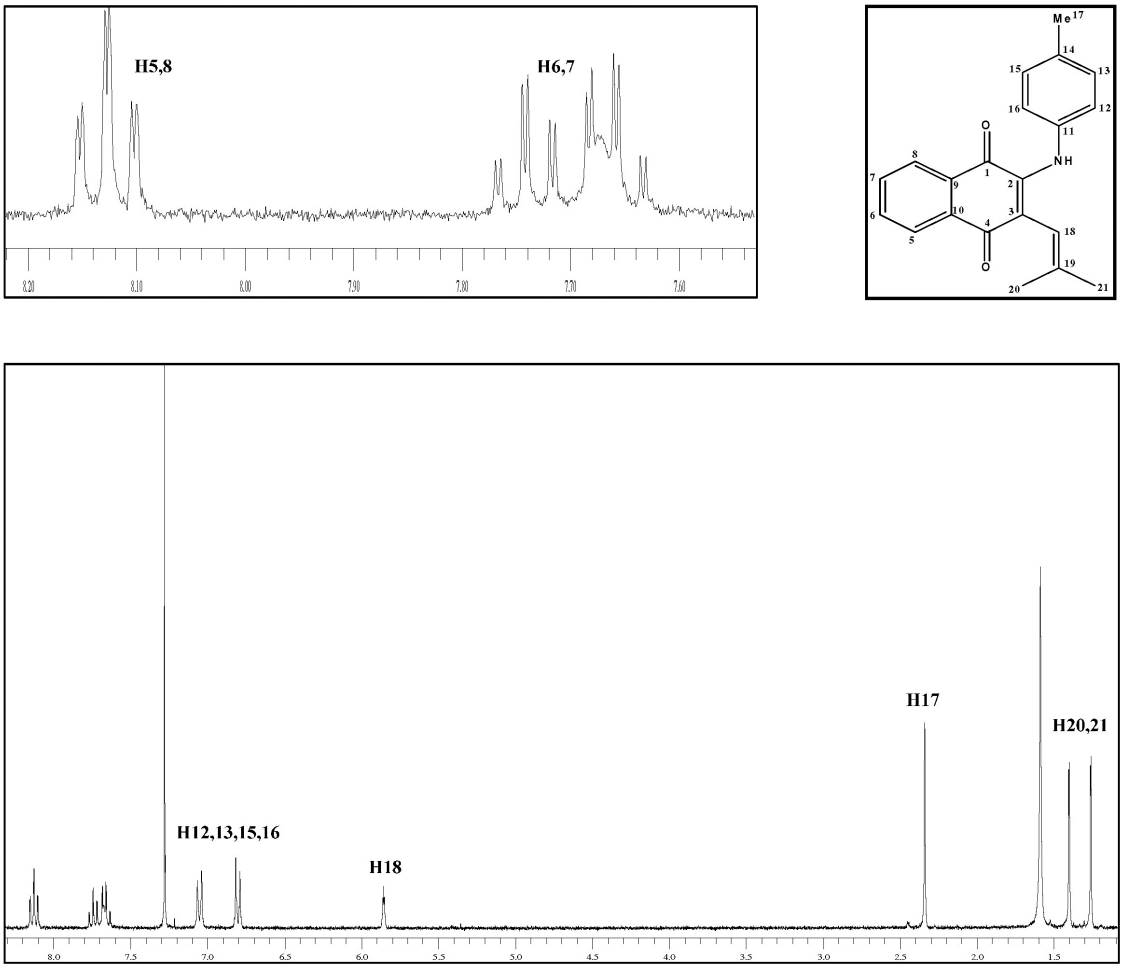

Figure S10. ^{1}H NMR spectrum of 2-(4-methyl-phenyl)amino-3-(2-methylpropenyl)-1,4-naphthoquinone (**2d**).

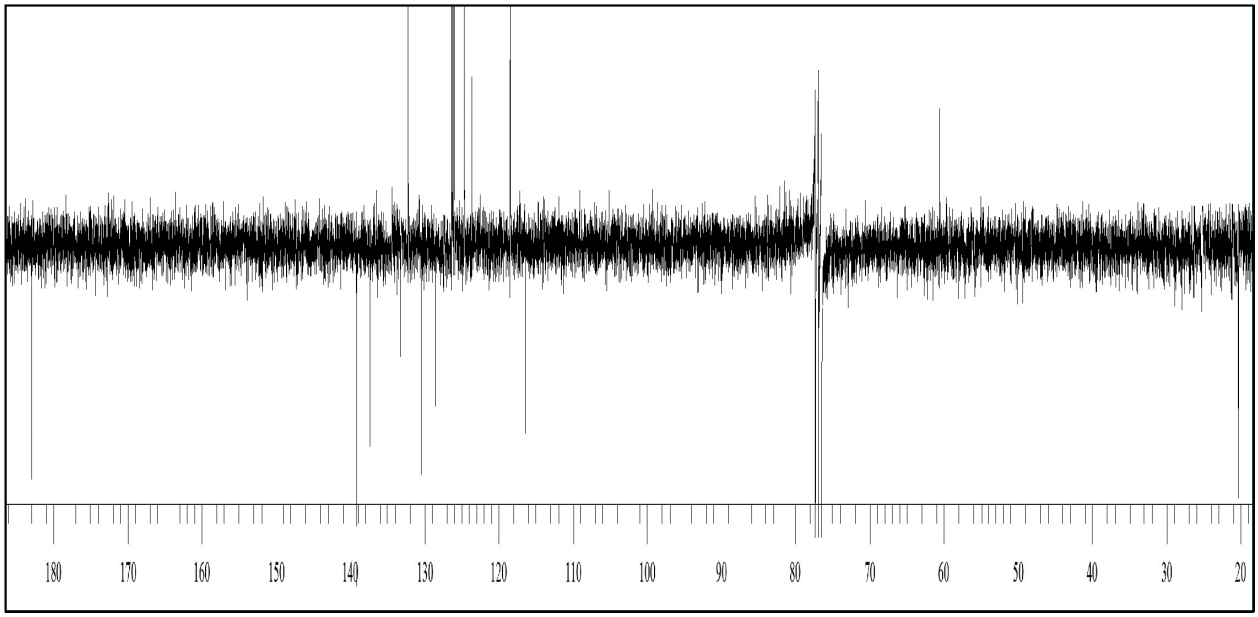

Figure S11. APT spectrum of 2-(4-methylphenyl)amino-3-(2-methylpropenyl)-1,4-naphthoquinone (**2d**).

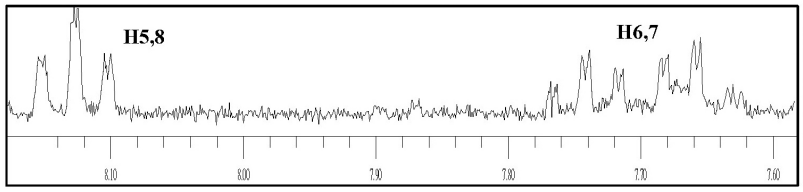

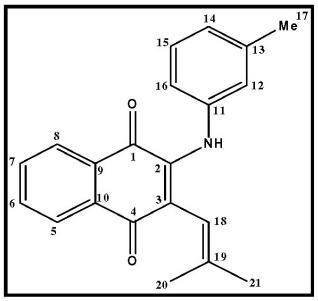

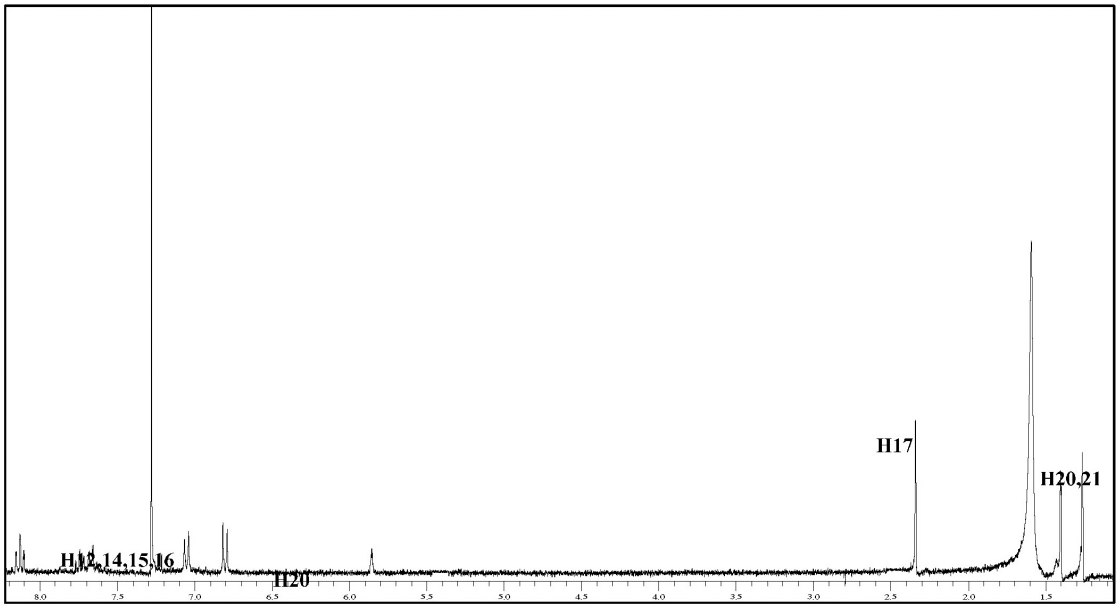

Figure S12. ^{1}H NMR spectrum of 2-(3-methylphenylene)amino-3-(2-methylpropenyl)-1,4-naphthoquinone (**2e**).

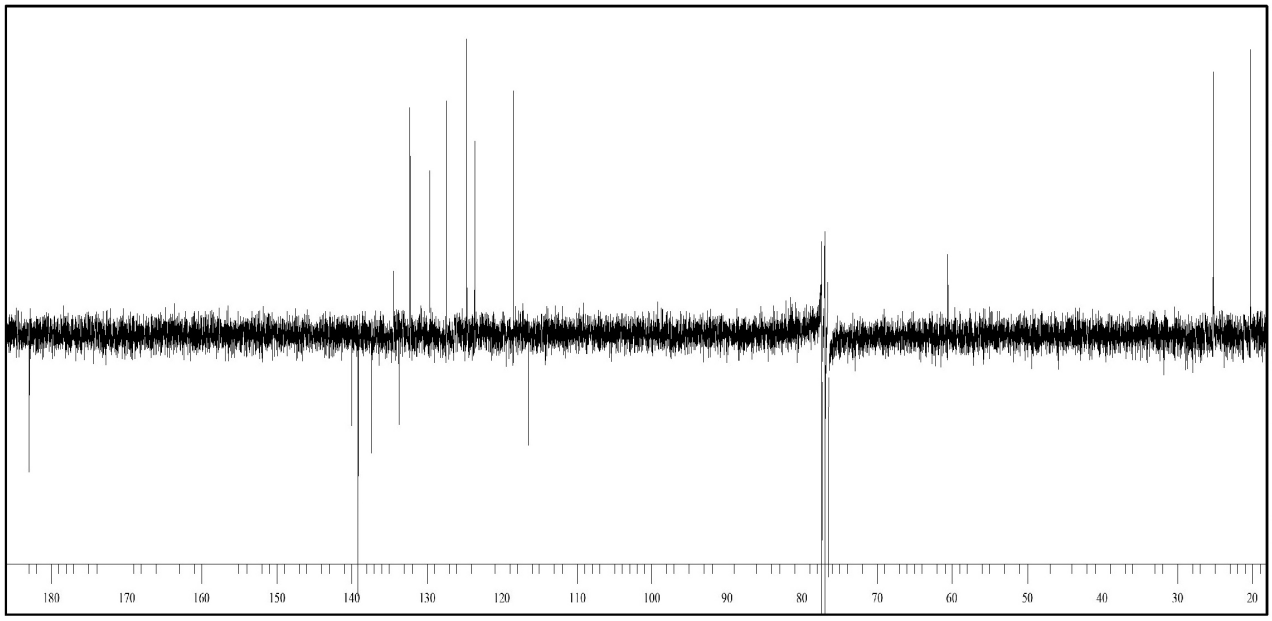

Figure S13. APT spectrum of 2-(3-methyl-phenyl)amino-3-(2-methylpropenyl)-1,4-naphthoquinone (**2e**).

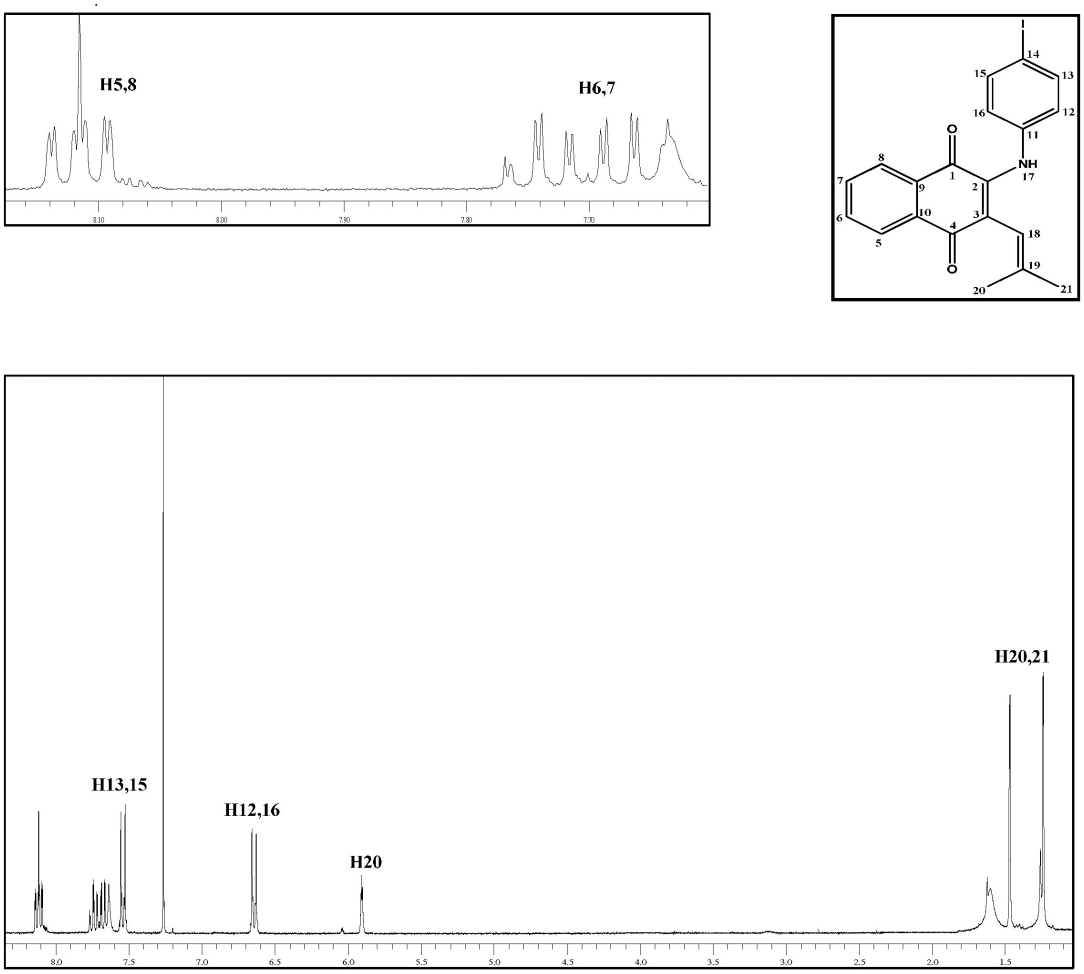

Figure S14. ^{1}H NMR spectrum of 2-(4-iodo-phenyl)amino-3-(2-methylpropenyl)-1,4-naphthoquinone (**2f**).

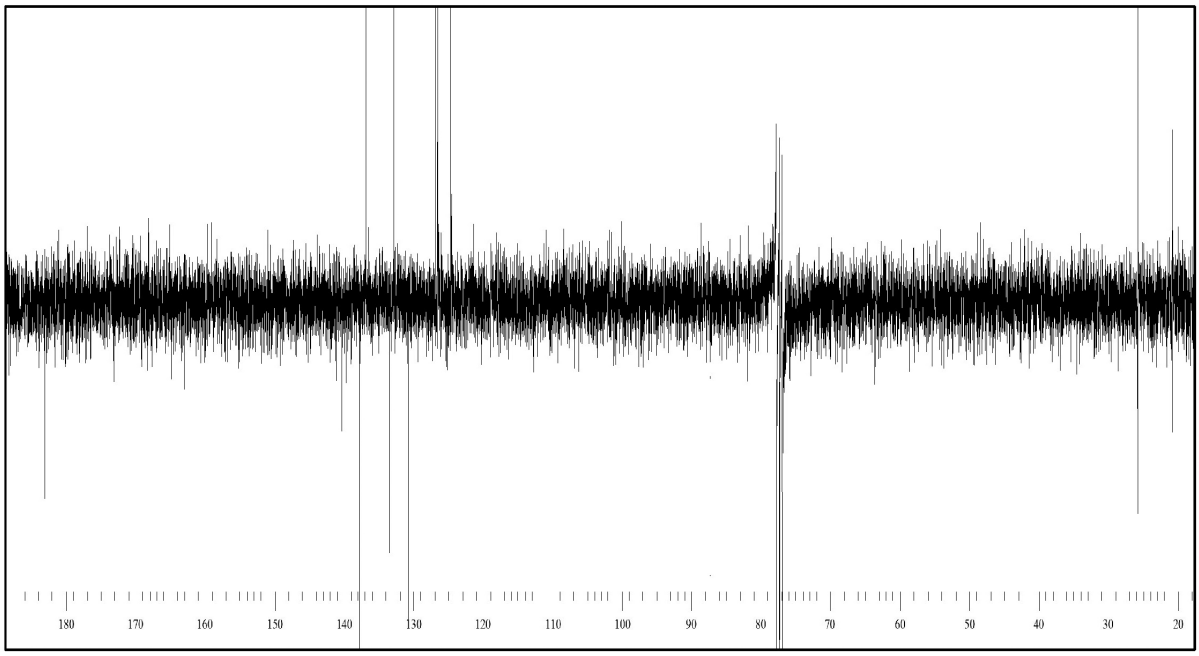

Figure S15. APT spectrum of 2-(4-iodo-phenyl)amino-3-(2-methylpropenyl)-1,4-naphthoquinone (**2f**).

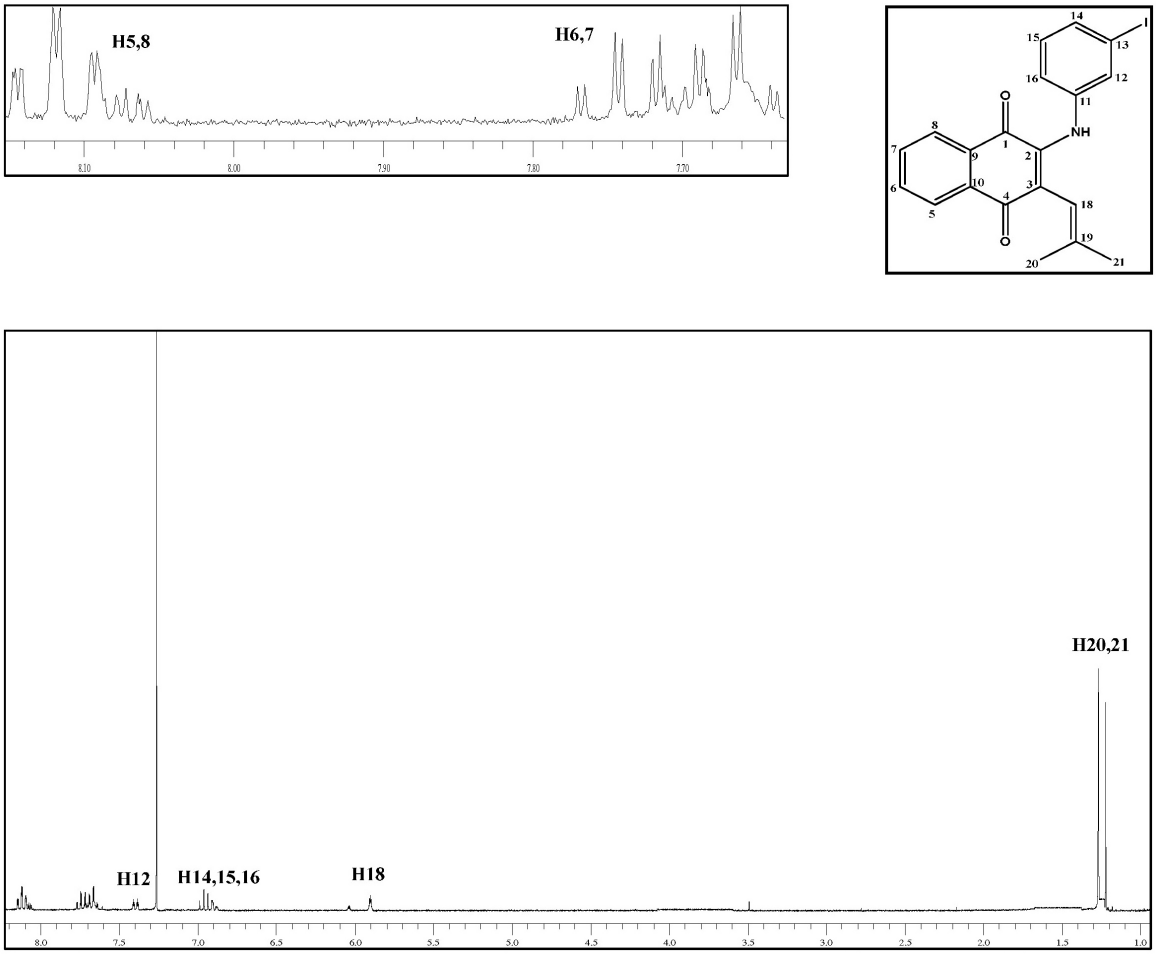

Figure S16. ^{1}H NMR spectrum of 2-(3-iodo-phenyl)amino-3-(2-methylpropenyl)-1,4-naphthoquinone (**2g**).

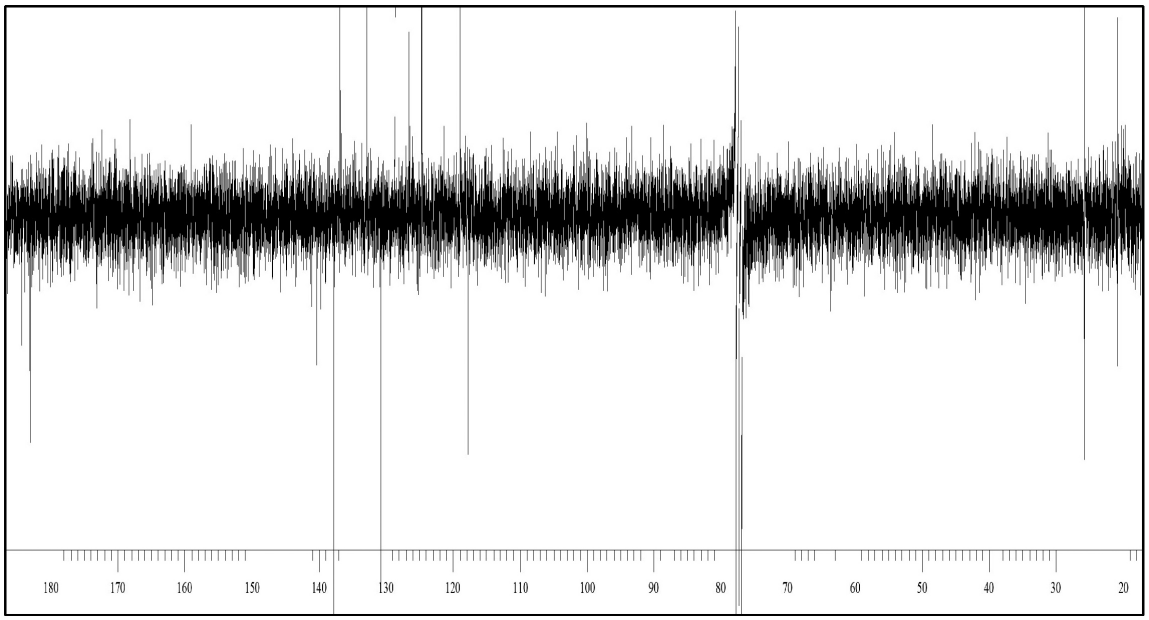

Figure S17. APT spectrum of 2-(3-iodo-phenyl)amino-3-(2-methylpropenyl)-1,4-naphthoquinone (**2g**).

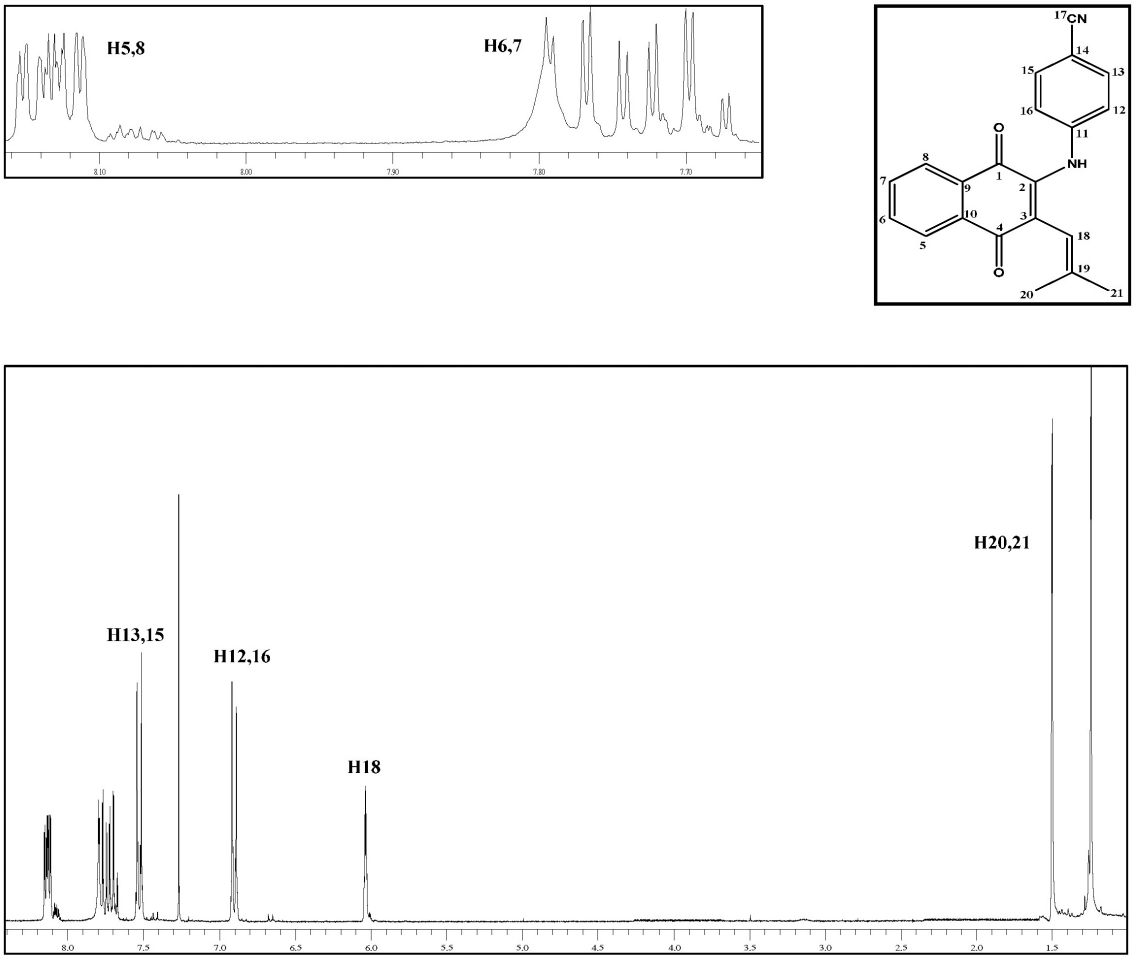

Figure S18. ^{1}**H NMR** spectrum of 2-(4-ciano-phenyl)amino-3-(2-methylpropenyl)-1,4-naphthoquinone (**2h**).

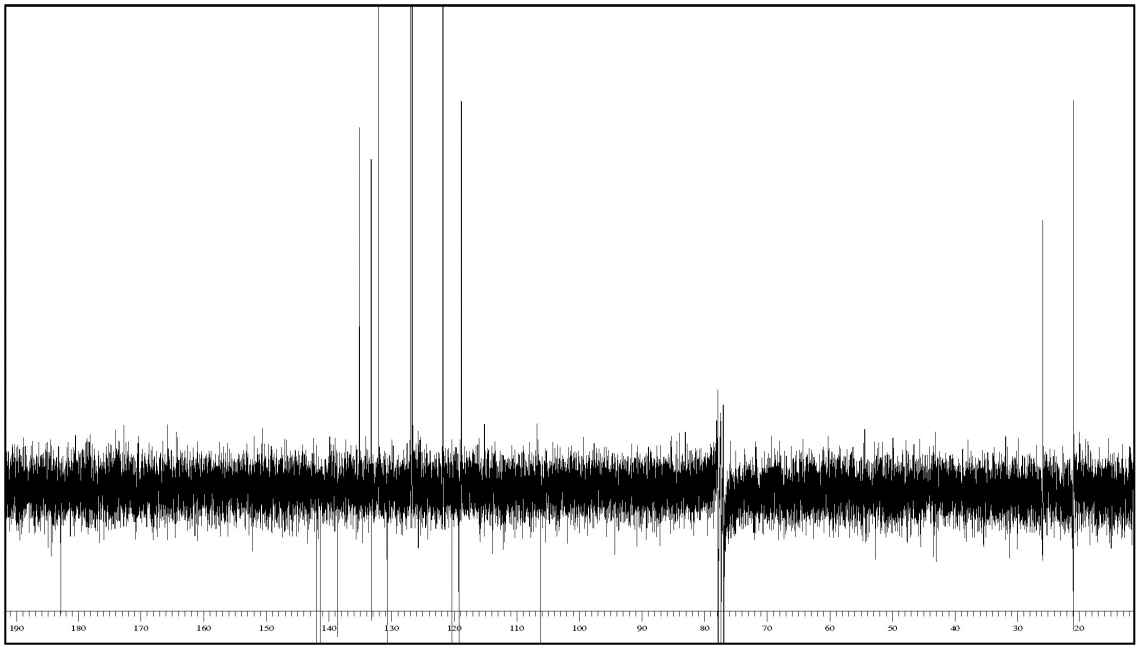

Figure S19. APT spectrum of 2-(4-ciano-phenyl)-3-(2-methylpropenyl)-1,4-naphthoquinone (**2h**).

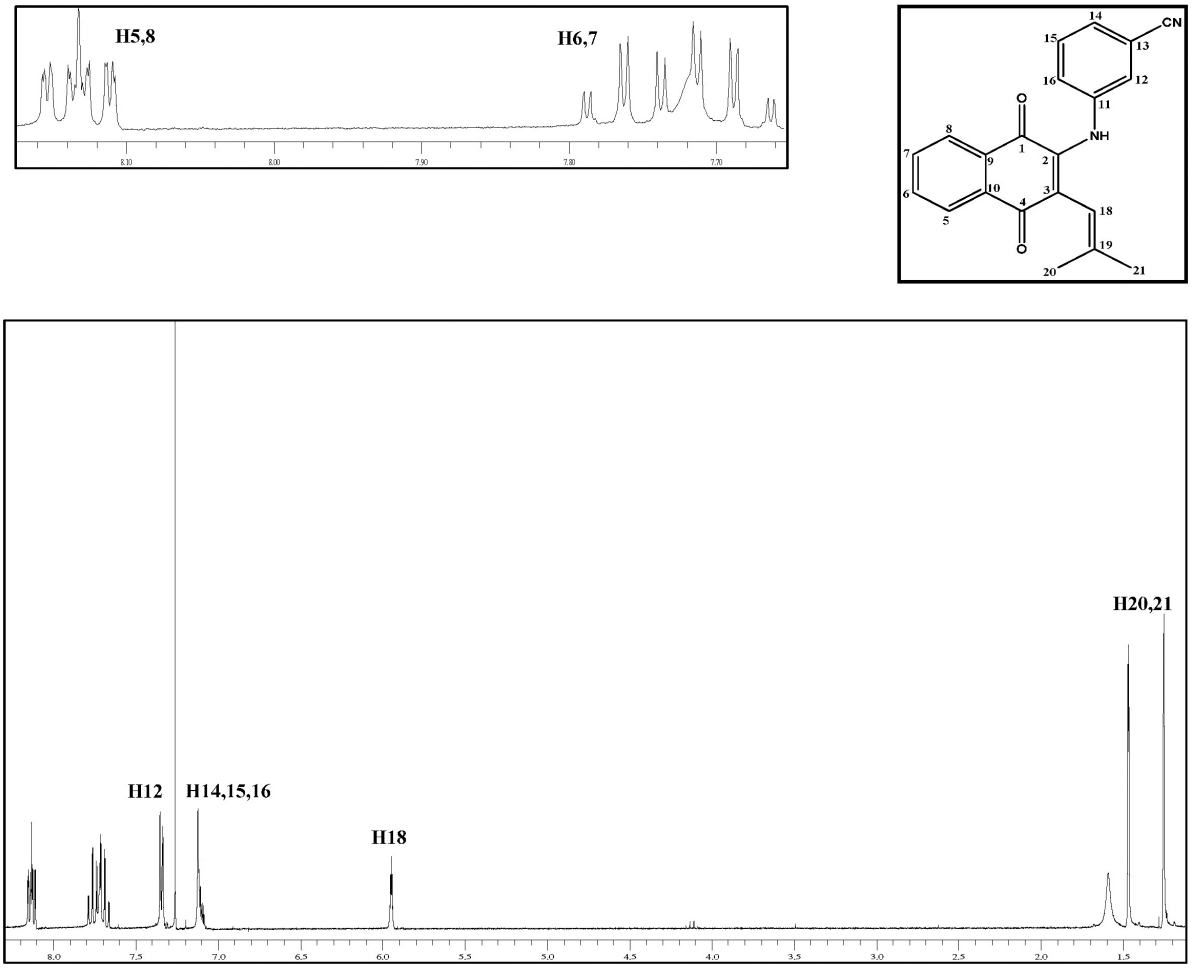

Figure S20. ^{1}H NMR spectrum of 2-(3-ciano-phenyl)amino-3-(2-methylpropenyl)-1,4-naphthoquinone (**2i**).

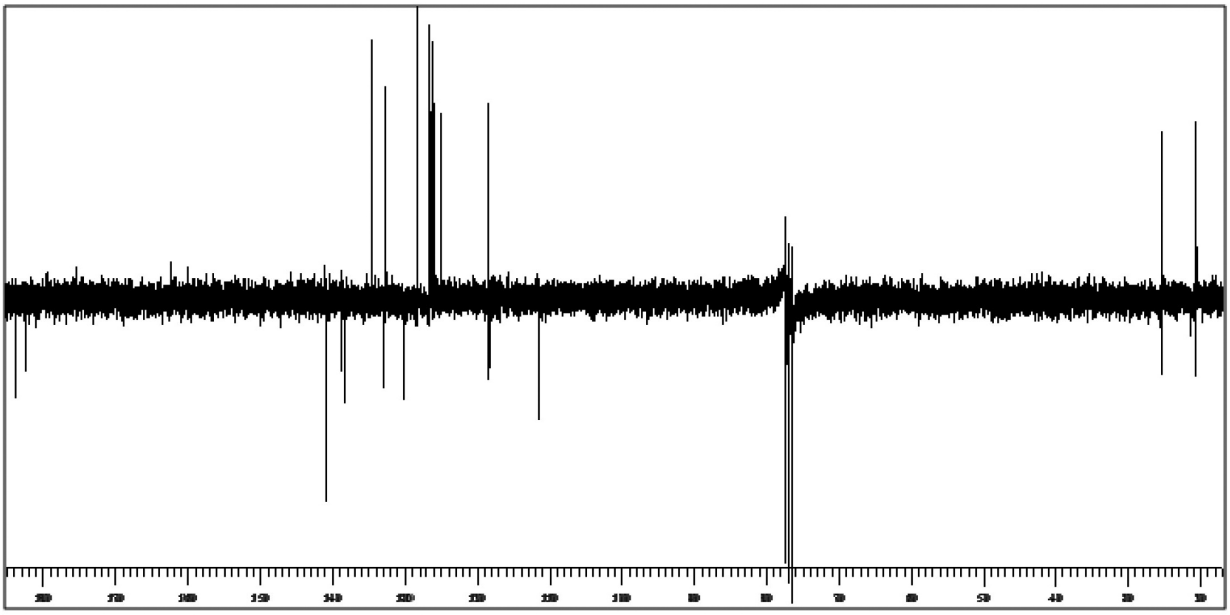

Figure S21. APT spectrum of 2-(3-ciano-phenyl)amino-3-(2-methylpropenyl)-1,4-naphthoquinone (**2i**).

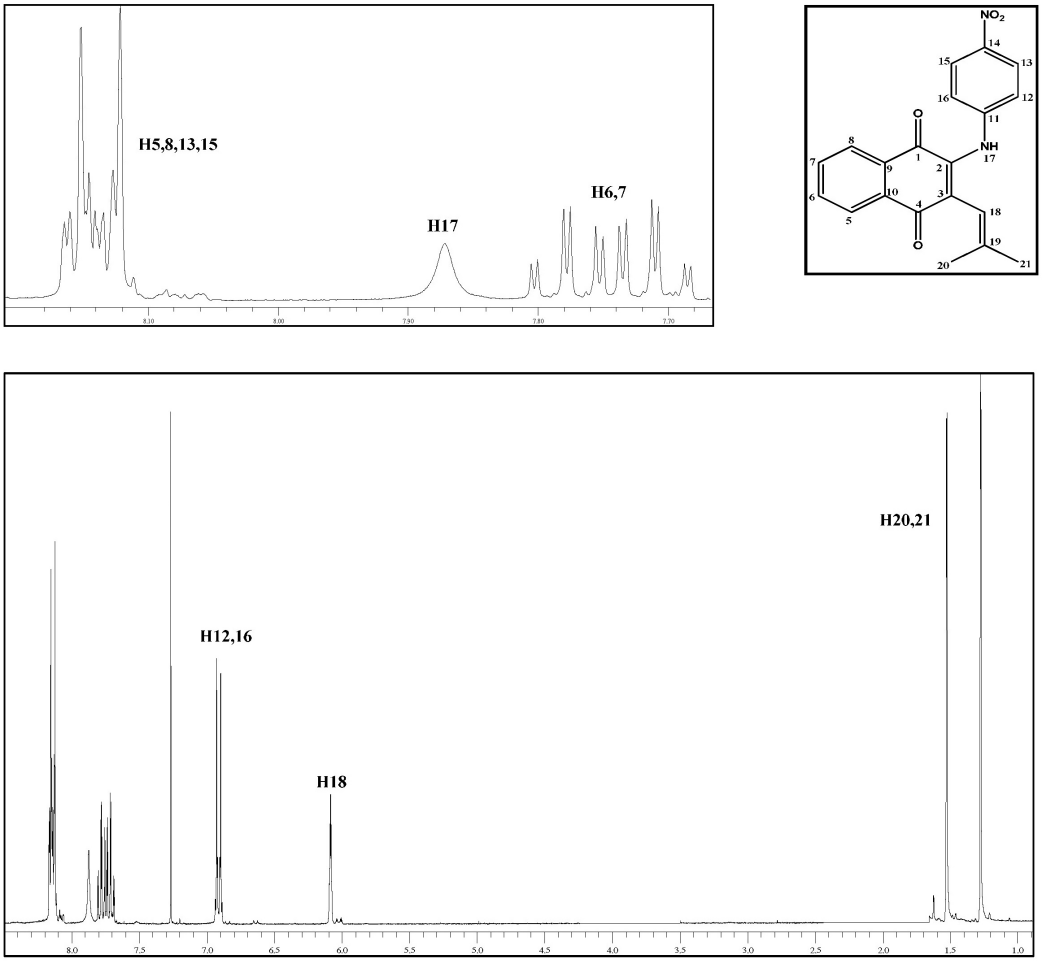

Figure S22. ^{1}**H NMR** spectrum of 2-(4-nitro-phenylene)-3-(2-methylpropenyl)-1,4-naphthoquinone (**2j**).

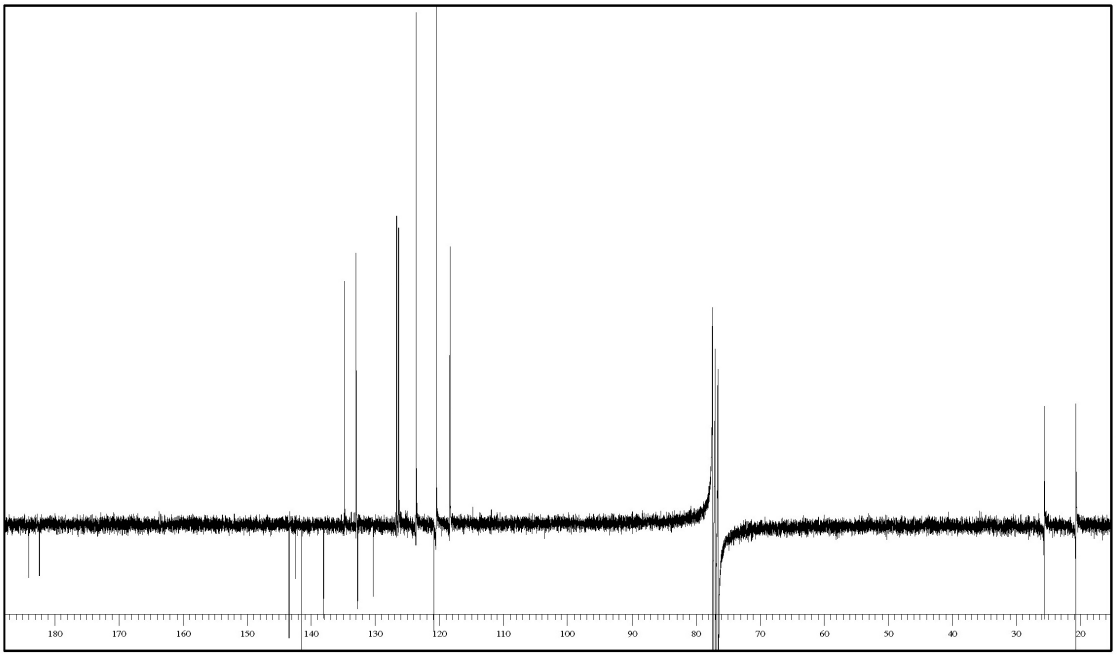

Figure S23. APT spectrum of 2-(4-nitro-phenyl)amino-3-(2-methylpropenyl)-1,4-naphthoquinone (**2j**).

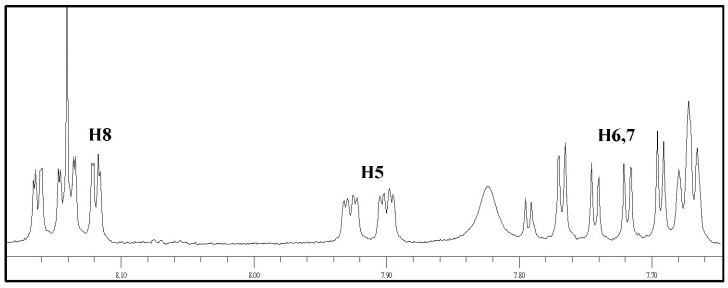

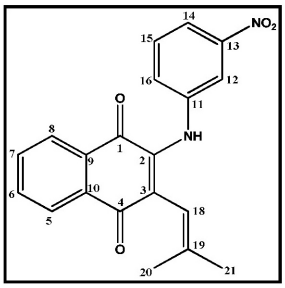

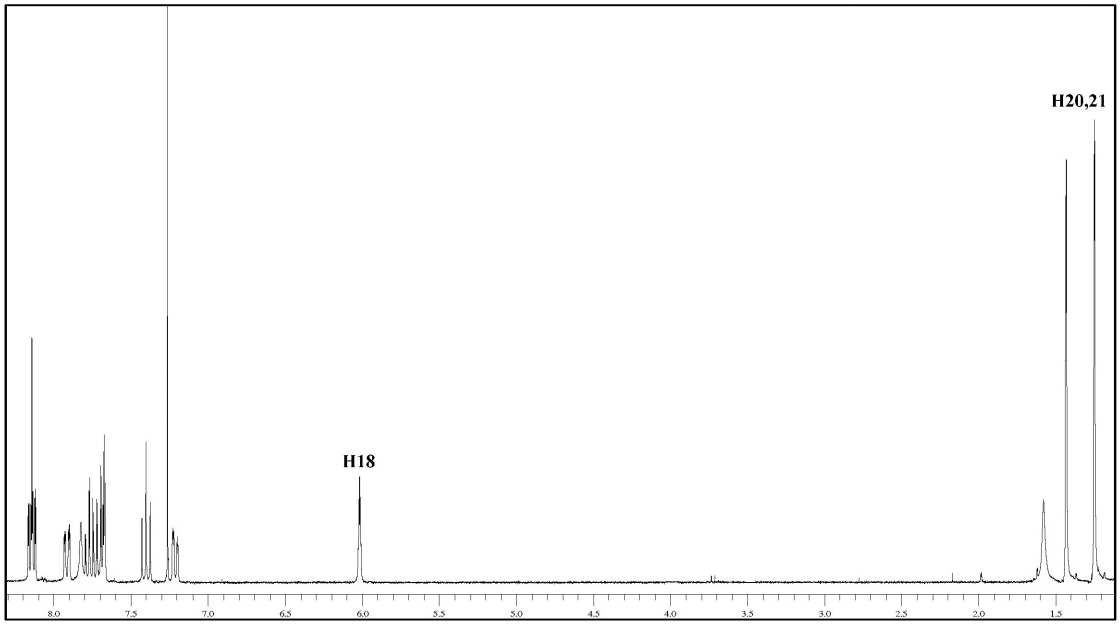

Figure S24. ^{1}H NMR spectrum of 2-(3-nitro-phenyl)amino-3-(2-methylpropenyl)-1,4-naphthoquinone (**2k**).

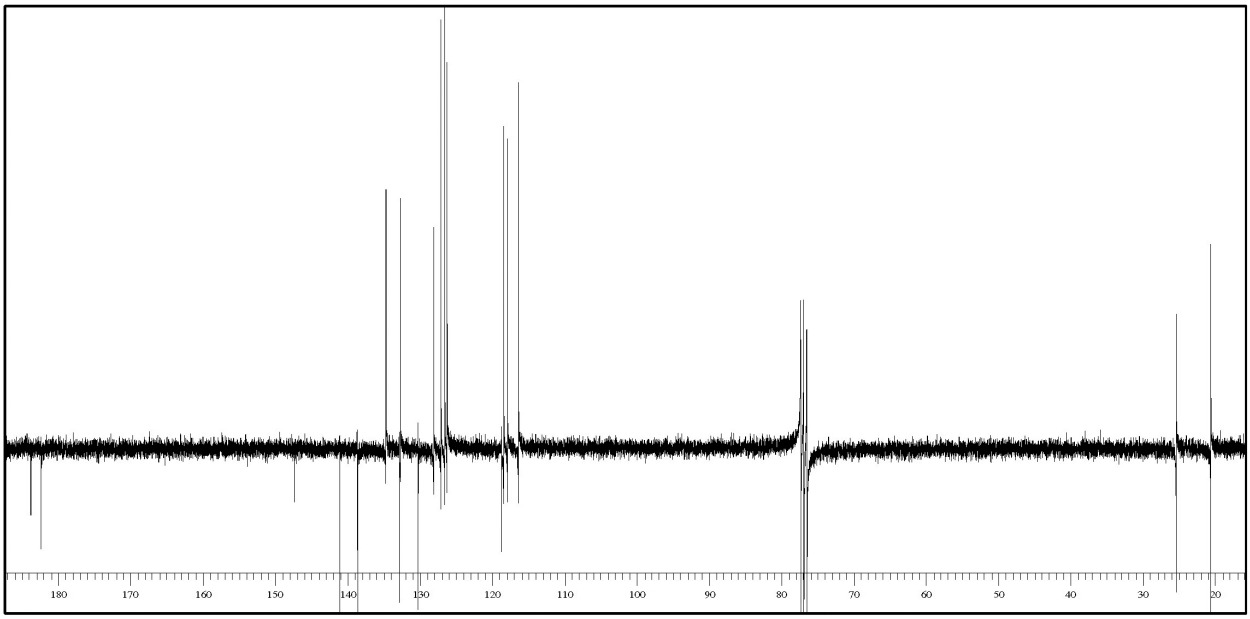

Figure S25. APT spectrum of 2-(3-nitro-phenyl)amino-3-(2-methylpropenyl)-1,4-naphthoquinone (**2k**).

4. Variable Temperature ^{1}H NMR Spectra of Compound 2a

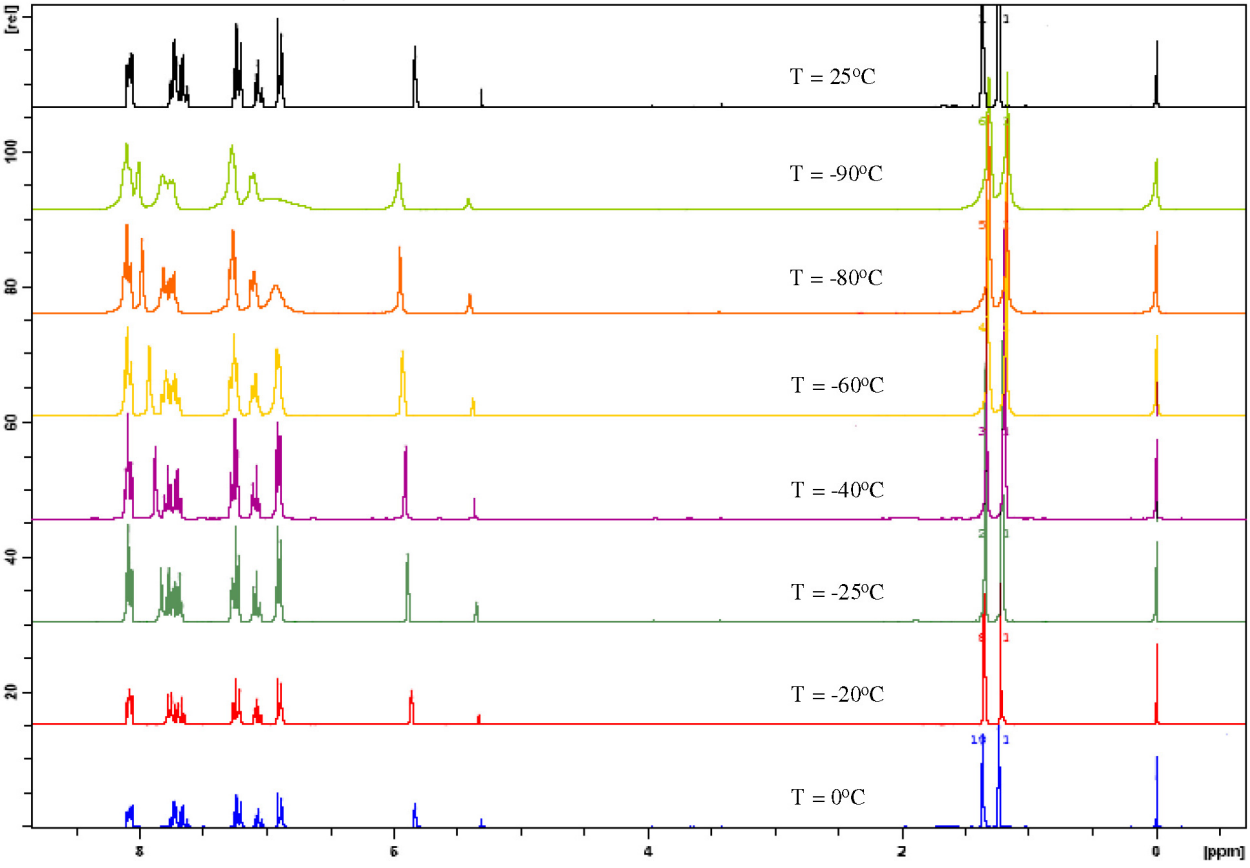

Figure S26. VT ^{1}H NMR spectra of compound **2a** (range: 25ºC to –90 ºC) in CD_2Cl_2.

4. Cyclic Voltammograms (100mV) of Compounds 2a-k

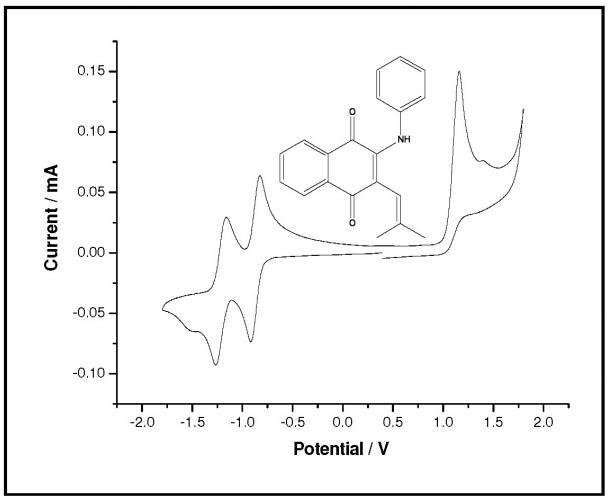

Figure S27. CV of 2-(phenyl)amino-3-(2-methylpropenyl)-1,4-naphthoquinone (**2a**).

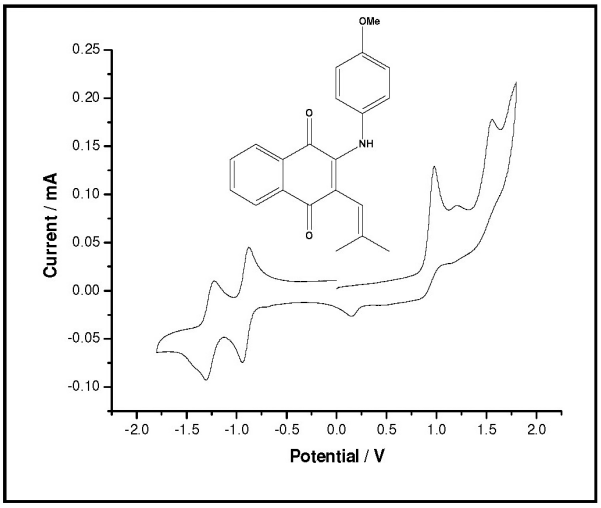

Figure S28. CV of 2-(4-methoxy-phenyl)amino-3-(2-methylpropenyl)-1,4-naphthoquinone (**2b**).

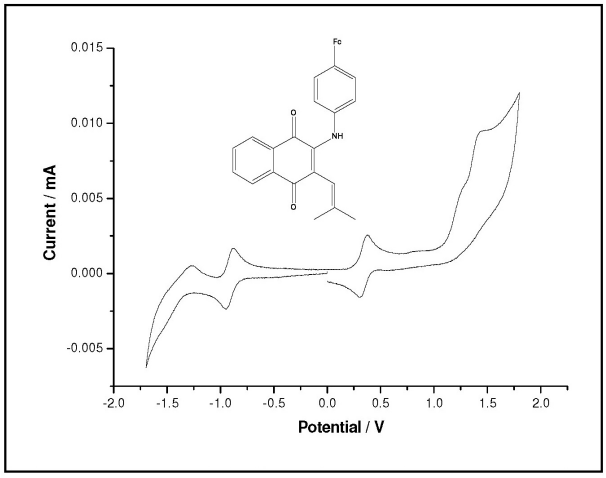

Figure S29. CV of 2-(4-ferrocenyl-phenyl)amino-3-(2-methylpropenyl)-1,4-naphthoquinone (**2c**).

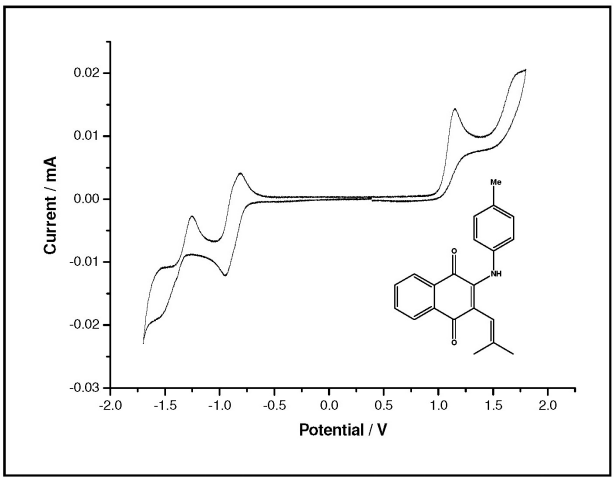

Figure S30. CV of 2-(4-methyl-phenyl)amino-3-(2-methylpropenyl)-1,4-naphthoquinone (**2d**).

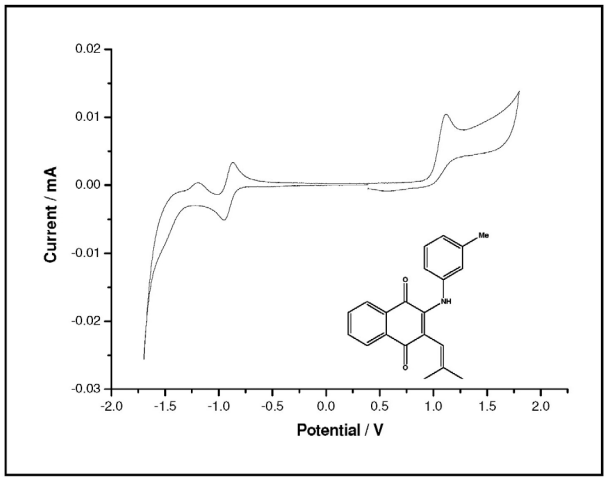

Figure S31. CV of 2-(3-methyl-phenyl)amino-3-(2-methylpropenyl)-1,4-naphthoquinone (**2e**).

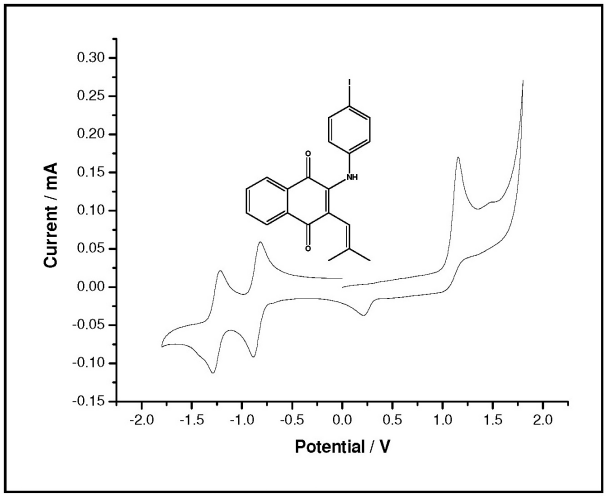

Figure S32. CV of 2-(4-iodo-phenyl)amino-3-(2-methylpropenyl)-1,4-naphthoquinone (**2f**).

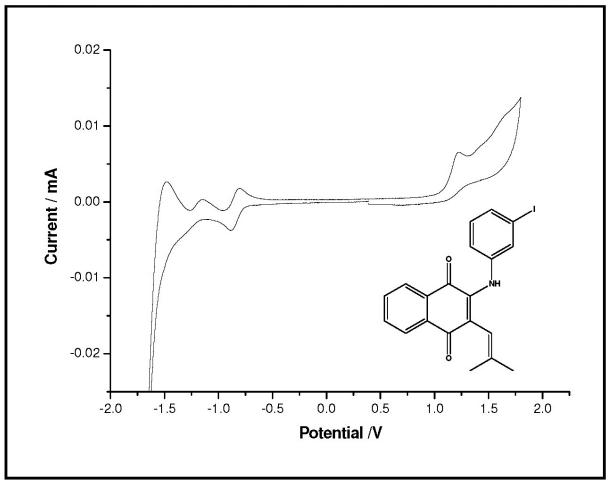

Figure S33. CV of 2-(3-iodo-phenyl)amino-3-(2-methylpropenyl)-1,4-naphthoquinone (**2g**).

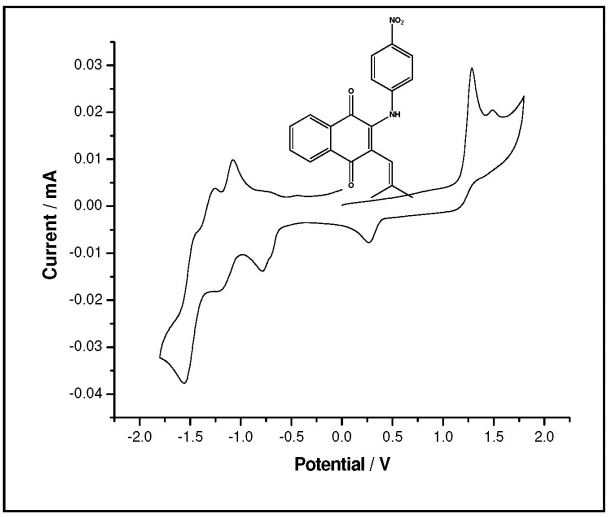

Figure S36. CV of 2-(4-nitro-phenyl)amino-3-(2-methylpropenyl)-1,4-naphthoquinone (**2j**).

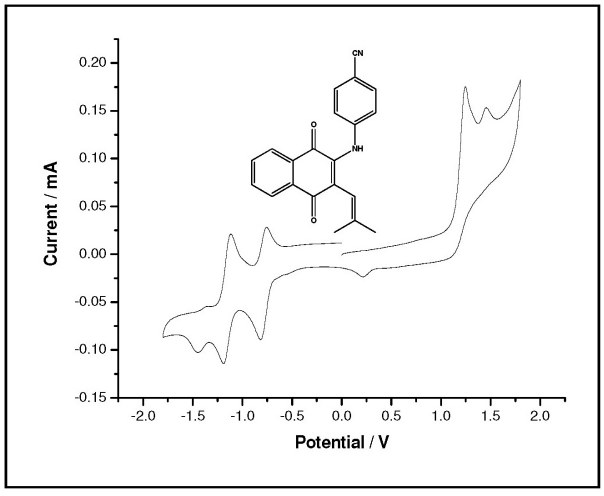

Figure S34. CV of 2-(4-ciano-phenyl)amino-3-(2-methylpropenyl)-1,4-naphthoquinone (**2h**).

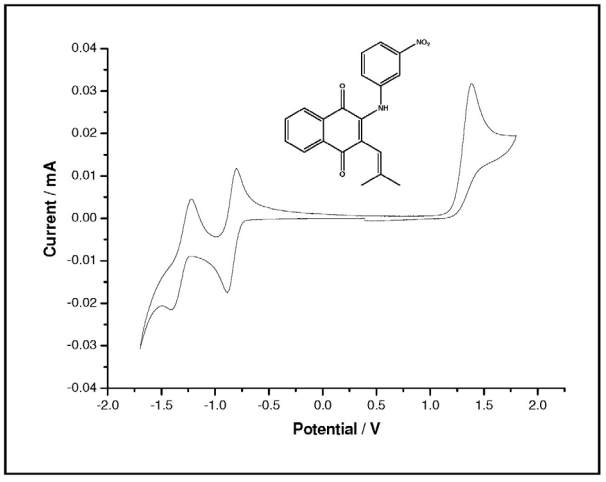

Figure S37. CV of 2-(3-nitro-phenyl)amino-3-(2-methylpropenyl)-1,4-naphthoquinone (**2k**).

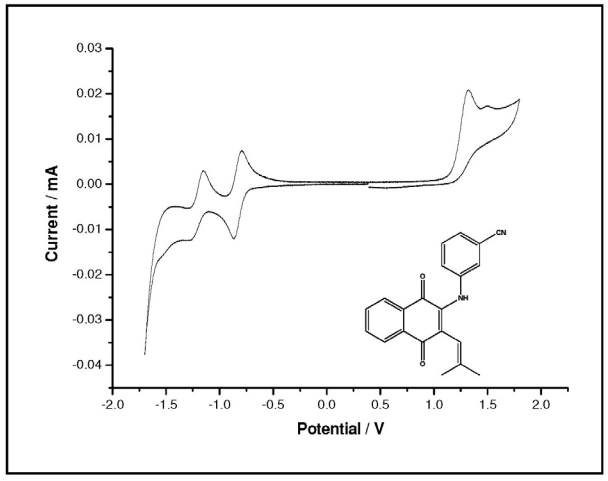

Figure S35. CV of 2-(3-ciano-phenyl)amino-3-(2-methylpropenyl)-1,4-naphthoquinone (**2i**).

5. Antitumor Assays

The antitumor screening of compounds **2a-k** was carried out against three cancer cell lines: SF-295 (central nervous system), HCT-8 (colon), MDAMB-435 (breast) through an MTT assay[ref] and the results are summarized in Table S6.

Table S6. Screening of the cytotoxic activity (growth inhibition %) of compounds **2a-k** and **1**

Compounds	SF295	GI%	HCT-8	GI%	MDA-MB435	GI%
	Average	SD	Average	SD	Average	SD
2a (H)	68.20	4.80	73.75	1.68	54.20	5.00
2b (4-OMe)	-11.01	11.89	-2.95	13.01	24.54	9.15
2c (4-Fc)	2.57	7.43	5.45	6.24	**102.31**	1.09
2d (4-Me)	12.20	3.71	12.33	2.76	17.21	3.58
2e (3-Me)	58.59	0.40	71.52	1.01	43.86	3.54
2f (4-I)	-4.93	23.88	10.29	2.13	-7.63	3.42
2g (3-I)	2.49	2.20	15.92	4.49	25.14	13.42
2h (4-CN)	-5.79	0.56	2.65	0.84	10.72	0.93
2i (3-CN)	-12.56	2.48	6.73	6.36	-20.51	4.35
2j (4-NO_2)	8.78	0.90	17.00	1.44	-18.20	8.24
2k (3-NO_2)	-7.40	4.20	17.03	2.02	4.01	7.68
1	41.09	15.08	27.01	3.12	**106.05**	0.16
DOX	96.19	0.63	94.85	3.99	**95.38**	2.23

DOX = positive control, doxorubicin.